

## THE INFLUENCE OF THE HEAT TREATMENT ON DELTA FERRITE TRANSFORMATION IN AUSTENITIC STAINLESS STEEL WELDS

Received – Prispjelo: 2011-05-19  
Accepted – Prihvaćeno: 2011-08-10  
Preliminary note – Prethodno priopćenje

Shielded metal arc (SMAW) welded specimens using austenitic consumable materials with different amount of delta-ferrite are annealed in range 650-750 °C through 2-10 hours. Factorial plan 3<sup>3</sup> with influenced factors regression analyse of measured delta-ferrite values is used. The transformation i.e. decomposition of delta ferrite during annealing was analysed regarding on weld cracking resistance using metallographic examination and WRC-1992 diagram.

*Key words:* SMAW, austenitic stainless steel welds, delta-ferrite transformation, heat treatment by annealing, metallographic examination.

**Utjecaj toplinske obradbe na pretvorbu delta-ferita u zavarima austenitnih nerđajućih čelika.** Ručno elektrolučno (REL) zavareni uzorci uporabom austenitnog korozivski postojanog dodatnog materijala s različitim udjelima delta ferita, žareni su u području 650-750 °C tijekom 2-10 sati. Korišten je faktorski plan 3<sup>3</sup> sa regresijskom analizom utjecajnih čimbenika mjerenih vrijednosti delta ferita. Pretvorba odnosno raspad delta ferita za vrijeme žarenja analizirana je s obzirom na otpornost zavara pukotinama metalografski i uporabom WRC-1992 dijagrama.

*Gljučne riječi:* REL, austenitni korozivski postojani zavari, pretvorba delta-ferita, toplinska obradba žarenjem, metalografsko ispitivanje.

### INTRODUCTION

In austenitic A mode stainless steels welds, according to Koseki at al [1], the interdendritic regions are enriched in Cr and Ni, while in AF mode weld metal occurs significant enrichment of Cr and depletion of Ni. Ferrite nucleates in the Cr-rich and Ni-depleted regions as a non-equilibrium phase. When FA and F mode solidification takes place, the dendrite core is significantly enriched in Cr and depleted in Ni. The segregation of Cr to ferrite and Ni to austenite during solidification plays a major role in stabilizing the ferrite during subsequent solid state transformation. The various ferrite morphologies observed at room temperature can be interpreted often only in terms of the solidification mode and the subsequent solid state transformation from ferrite to austenite (Figure 1). The change in composition can be considered in terms of Cr<sub>eq</sub>/Ni<sub>eq</sub> ratio [2]. For higher Cr<sub>eq</sub>/Ni<sub>eq</sub>, AF mode solidification occurs in which austenite is the primary phase. For low ratios, A-mode solidification occurs and there is no change in structure after solidification as no ferrite is present and a part of the remaining liquid solidifies as intercellular ferrite.

On cooling to lower temperatures, most of the ferrite transforms and the residual ferrite left behind in the Cr-rich dendritic cores causing the characteristic structure known as vermicular ferrite. For still higher Cr<sub>eq</sub>/Ni<sub>eq</sub>

ratios in the FA and F modes, the ferrite is increasingly stable and the  $\delta \rightarrow \delta + \gamma$  phase boundary occurs lower in temperature. As the transformation kinetics become slow, elongated acicular and Widmanstätten type morphologies are promoted. Solidification cracking occurs predominantly by the segregation of solutes to form lowmelting phases, which under the action of shrinkage stresses close to solidification cause cracking.

The tendency of weld solidification cracking decreases dramatically at Cr<sub>eq</sub>/Ni<sub>eq</sub> ratios slightly less than 1,5 for equivalence determined from WRC-1992 calculations, as shown in Figure 2. [3]

The Cr<sub>eq</sub> and Ni<sub>eq</sub> are calculated corresponding to the equations empirically derived from the WRC-1992 equation and then plotted on the appropriate constitution diagram to determine which microconstituent will initially solidify [2, 4].

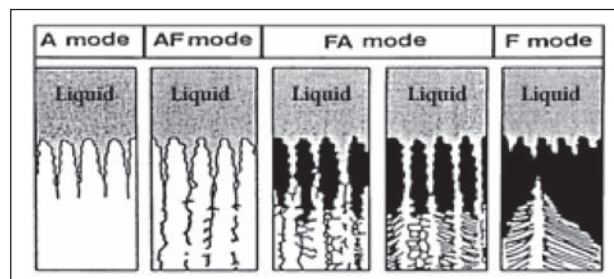


**Figure 1** Schema of solidification modes in austenitic stainless steelwelds with phase morphologies [1]

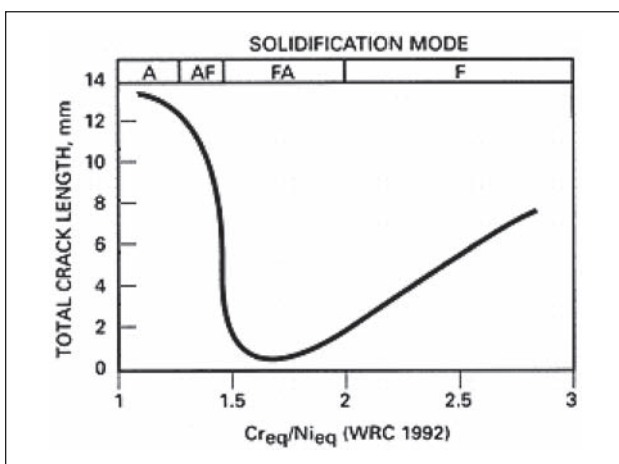


Figure 2 Cracking susceptibility based on WRC-1992 Creq and Nieq [3]

### EXPERIMENTS

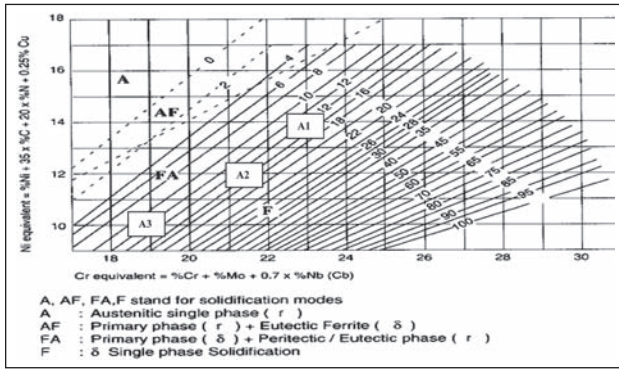
Shielded metal arc (SMA) welded specimens are submitted to annealing in range 650-750 °C. Sensibilization time is varied in range 0 - 10 hours. The specimens are welded with austenitic filler metals containing different amount of delta-ferrite with chemical composition shown in Table 1. Delta-ferrite contents in dissimilar austenitic welds are determined by dr. Foerster-Institute Ferrite Content - Meter type 1,054 device which work on magnetic permeability basis. Measuring was performed on six different places of specimens dimensions 22 × 6 × 4 mm and on minimum three (3) specimens for each level of experiment. On Figure 3, WRC-1992 diagram is shown with location of predicted weld metal composition calculated from chemical analysis of used filler metals. Review of delta ferrite values measured on welds specimens with joint-macrostructure shown on picture is presented on Table 2. The table

Table 1 Chemical elements analysis of SMAW consumable material

SMAW consumable material	Elements content, wt / %								
	C	Si	Mn	Ni	Cr	Mo	S	P	Fe
A1 AWS E 309 L	0,019	0,85	0,83	13,3	23,3	-	0,011	0,022	Rem.
A2 AWS E 316 L	0,019	1,03	0,55	11,0	18,8	2,82	0,003	0,023	Rem.
A3 AWS E 308 L	0,030	0,80	0,60	9,20	19,1	-	0,060	0,060	Rem.

Table 2 Review of average values  $\bar{X}$  of  $\delta$ -ferrite measured in welds with regression equations

Consumable SMAW material A 	Annealing time / hours C Annealing temperature/°C B	C <sub>1</sub> = 0 hours No annealing		C <sub>2</sub> = 2 hours		C <sub>3</sub> = 10 hours		Regressions Equations
		$\bar{X}$	min-max	$\bar{X}$	min-max	$\bar{X}$	min-max	
A <sub>1</sub> AWS E 309 L Creq./Nieq.=1,668 (WRC-1992)	B <sub>1</sub> 650 °C	5,00 4,85 3,90	$\bar{X}$ =4,58	2,25 2,30 2,50	$\bar{X}$ =2,37	0,15 2,25 3,10	$\bar{X}$ =1,84	$\delta$ -ferit = 3,595- -0,000056B- -0,269 C
	B <sub>2</sub> 700 °C	5,00 4,85 3,90	$\bar{X}$ =4,58	1,35 1,70 1,25	$\bar{X}$ =1,44	1,55 1,05 1,05	$\bar{X}$ =0,22	
	B <sub>3</sub> 750 °C	5,00 4,85 3,90	$\bar{X}$ =4,58	0,80 1,75 1,70	$\bar{X}$ =1,42	0,45 0,30 0,20	$\bar{X}$ =0,32	
A <sub>2</sub> AWS E 316 L Creq./Nieq.=1,853 (WRC-1992)	B <sub>1</sub> 650 °C	6,35 6,20 5,75	$\bar{X}$ =6,10	3,35 3,20 2,85	$\bar{X}$ =3,1	0,45 3,80 3,35	$\bar{X}$ =2,53	$\delta$ -ferit = 5,6299- -0,00156B- -0,3148 C
	B <sub>2</sub> 700 °C	6,35 6,20 5,75	$\bar{X}$ =6,10	2,18 2,60 1,35	$\bar{X}$ =2,04	2,80 3,10 1,40	$\bar{X}$ =2,43	
	B <sub>3</sub> 750 °C	6,35 6,20 5,75	$\bar{X}$ =6,10	0,75 0,75 0,95	$\bar{X}$ =0,82	0,40 0,40 0,45	$\bar{X}$ =0,42	
A <sub>3</sub> AWS E 308 L Creq./Nieq.=1,863 (WRC-1992)	B <sub>1</sub> 650 °C	2,35 3,45 2,15	$\bar{X}$ =2,65	2,30 2,50 3,35	$\bar{X}$ =2,72	3,00 3,60 2,70	$\bar{X}$ =3,1	$\delta$ -ferit = 2,526- -0,00011B- -0,0649 C
	B <sub>2</sub> 700 °C	2,35 3,45 2,15	$\bar{X}$ =2,65	1,25 2,05 2,25	$\bar{X}$ =1,85	2,15 1,40 1,15	$\bar{X}$ =1,57	
	B <sub>3</sub> 750 °C	2,35 3,45 2,15	$\bar{X}$ =2,65	2,10 0,85 1,95	$\bar{X}$ =1,63	0,95 0,85 0,85	$\bar{X}$ =0,88	



**Figure 3** WRC-1992 diagram with areas of expected austenitic weld structures regarding on cracking resistance using consumable materials A1; A2; A3.

presents regression equations and calculated Creq./Nieq. for each used filler metals, too. The characteristic diagrams on transformation-decomposition level of delta ferrite depending on start level (different type of austenitic filler metals), annealing temperature (sensibilisation range) and annealing time are presented on Figures 4 and 5. Delta - ferrite microstructure-morphology transforming of different austenitic welds depending on annealing parameters (temperature and time) is shown on Figure 6. Metallographical analysis of austenitic welds is performed by optical Leitz microscopy. Review of austenitic welds delta-ferrite structure is developed-electrolytically etched by 5 % KOH. All photographs are magnificated 500 x.

**DISCUSSION**

When hot cracking occurs in a austenite weld metal, a comon solution is to use a mostly austenite filler metal that includes a small amount of ferrite.

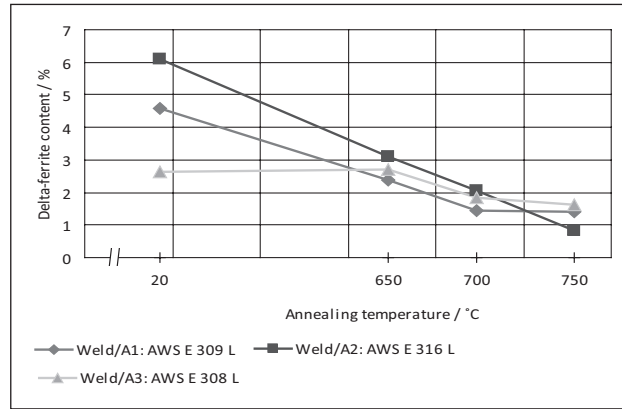


**Figure 4** Delta-ferrite transformation depending on annealing temperature during t=2 hours

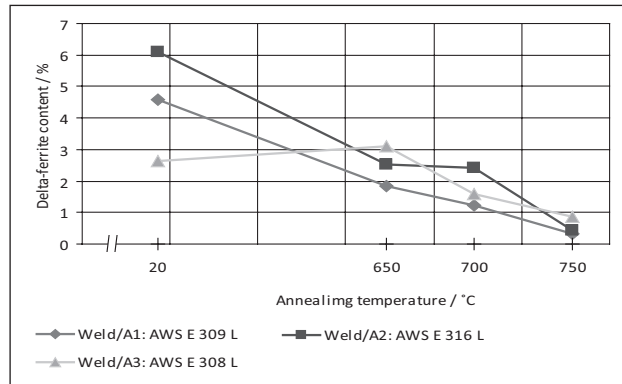


**Figure 5** Delta-ferrite transformation depending on annealing temperature during t=10 hours

However, another approach to avoiding hot cracking may be necessary in situations that require low magnetic permeability, high toughness at cryogenic temperatures, resistance to media that selectively attack ferrite (such as urea) or postweld heat treatments (PWHTs)

DELTA-FERRITE	B1C1(no anneal)	B1C2(650°C/2h)	B2C2(700 °C/2h)	B3C2(750 °C/2h)
A1 (AWS E309L) Creq./Nieq. = 1,668				
A2 (AWS E316L) Creq./Nieq.= 1,853				
A3 (AWS E 308L) Creq./Nieq. =1,863				

**Figure 6** Delta-ferrite morphology and transformation during heat treatment by annealing

that embrittle ferrite. These requirements have to strictly limit the acceptable amount of ferrite.

Because primary ferrite is the preferable microstructure, use of the WRC-1992 diagram should reduce problems of hot cracking during welding.

Although the WRC-1992 diagram is more accurate in predicting ferrite content for many weld metal, the Schaeffler diagram still retains some utility because it can offer reasonable accurate prediction in terms of martensite in low-alloyed stainless steel composition. This is because the WRC-1992 diagram does not include effect of Mn (manganese). Without manganese (Mn) effect, it is not possible to put a boundary for the martensite phase in the WRC-1992 diagram. The dashed-dividing line between compositions that solidify primary as austenite and that solidify primary as ferrite is not parallel to the isoferrite lines. It is at a small angle to isoferrite lines what means that more ferrite is necessary at room temperature to confirm presence of primary ferrite solidification in higher-alloyed than in low-alloyed stainless steel weld metals.

## CONCLUSIONS

The volume of delta-ferrite in used filler metal (WRC-1992 diagram) comparing with measuring values of delta-ferrite at performed austenitic stainless steel weld evidently dropped. Multipass welding, heat input, penetration and cooling rate caused decomposition of ( $\gamma+\delta$ ) structure. During the heat treatment by annealing the decomposition of delta-ferrite continues and reaches maximum at 750 °C through 10 hours. The largest drop registered at heat treated joints which was welded by austenitic electrodes with the highest FN.

Regression analysis directed on significantly influence of filler metals sorts i.e. chemical content or Creq./Nieq. rate. The influence of temperatures levels is minor comparing with influence of the time of duration. Regardless of all filler metal solidifies in AF mode (high resistance to cracking resistance), austenitic welds after performed heat treatment have low cracking resistance. The volume of delta-ferrite decreased by annealing including decomposition and transformation into carbides and intermetallic phases ( $\sigma$ -phase,  $\chi$ -phase) causing weld brittleness. Delta-ferrite morphology varied from vermicular, lacy and acicular shape to globular form at higher temperature and longer exposition time.

The heat treatment by annealing of austenitic weld has damaging influence on inclination to brittleness of austenitic welds with small amount of delta ferrite. Specially it is characteristically at austenitic welds with molybdenum.

## REFERENCES

- [1] T. Koseki, M.C. Flemings: Metallurgical Materials Transaction (1996), A27, : 3226 – 3240.
- [2] D.J.Kotecki, T.E.Siewert: Welding Journal, 71 (1992), 5, 171-178.
- [3] Welding Handbook, 8<sup>th</sup> Edition, Vol. 4, Materials and Applications, Part 2., AWS, Miami, FL. 1998.
- [4] D.L. Olson: Welding Journal, 64 (1985), 281- 295.
- [5] E. Folkhard : Metallurgie der Schweissung nichtrostender Staehle, Springer-Verlag, Wien, 1984.
- [6] B. Mateša: Zavarivanje, 34 (1991), 3/4, 67-75.
- [7] B. Mateša: Zavarivanje, 35 (1992), 1, 5-13.

**Note:** Responsible translator: Željka Rosandić, Faculty of Mechanical Engineering in Slavonski Brod, University of Osijek, Slavonski Brod, Croatia